Chapter 2
Nonlinear Modeling of Squeeze-Film Phenomena

in Microbeam MEMS

Reza N. Jazar

Abstract Oscillating microplates attached to microbeams is the main part of many microresonators and micro-electro-mechanical systems (*MEMS*). The sque-eze-film phenomena appears when the microplate is vibrating in a viscose medium. The phenomena can potentially change the design point and performance of the micro-system, although its effects on *MEMS* dynamic are considered secondary compared to main mechanical and electrical forces. In this investigation, we model the squeeze-film phenomena and present two nonlinear mathematical functions to define and model the restoring and damping behaviors of squeeze-film phenomena.

Accepting an analytical approach, we present the mathematical modeling of microresonator dynamic and develop effective equations to be utilized to study the electrically actuated microresonators. Then employing the averaging perturbation method, we determine the frequency response of the microbeam and examine the effects of parameters on the resonator's dynamics. The nonlinear model for *MEMS* includes the initial deflection due to polarization voltage, mid-plane stretching, and axial loads, as well as the nonlinear displacement coupling of the actuating electric force. The main purpose of this chapter is to present an applied model to simulate the squeeze-film phenomena, and introduce their design parameters.

2.1 Introduction and Background

This investigation presents two mathematical functions to describe stiffness and damping characteristics of squeeze-film phenomena. Micromechanical devices usually obey a complex set of equations of motion to model the tight coupling

R.N. Jazar (✉)
School of Aerospace, Mechanical, and Manufacturing Engineering, RMIT University, Melbourne, Victoria, Australia
e-mail: reza.jazar@rmit.edu.au

L. Dai and R.N. Jazar (eds.), *Nonlinear Approaches in Engineering Applications*,
DOI 10.1007/978-1-4614-1469-8_2, © Springer Science+Business Media, LLC 2012

of multiple energy domains of the system. Direct solution of these equations based on fully meshed structures is computationally intensive, making it difficult to use in system-level simulation. In order to perform rapid design prediction and optimization, accurate, and easy-to-use *reduced-order MEMS* device models must be built (Chen et al. 2004). In order to overcome the high computational cost problem and provide a fast and efficient system level simulation, the *MEMS* design community has converged to construct the low-order models. A common approach is based on parameterized lumped element representation for *MEMS* devices (Mukherjee et al. 1999; Fedder 1994).

Cantilevers have shown to be reliable structures for resonators, in both macro and micro scales. However, shrinking increases the strength-to-weight ratio and allows devices to be constructed with aspect ratios that would not be possible in the macro domain. Also, surface tension and viscous forces become increasingly significant at smaller dimensions (Madou 2002). These viscous forces present a challenge in observing the oscillation of the microbeams even at pressures of a few hundred m torr (Harmany 2003). Furthermore, when the beam deflection is large, the linearized model deviates from the device nonlinear model significantly. To overcome the difficulties of modeling the interactions of so many phenomena that are involved in *MEMS*, a reduced-order nonlinear model is necessary.

MEMS devices have mainly been designing by trial and error. As a result, *MEMS* design process requires several iterations before the required performance of a given device are satisfied. Experiments must be utilized to validate the theoretical prediction and clarify the order of contribution of the involved physical phenomena. Experimental results depend on the accuracy of the experimental devices and on the skills and knowledge of the experimenter. On the other hand, the *FEM* software are limited because they are time consuming, cumbersome, expensive, and they use numerous variables to represent the state of the system, where most of those variables are not important to the designer (Younis et al. 2003; Nayfeh and Younis 2004a,b). Conversely, the reduced-order models, known as *micromodels*, need to be expanded and improved as a basis for prediction and optimization tool of the proposed behavior. Reduced-order models are developed to capture the most significant characteristics of an *MEMS* behavior in a few variables (Younis et al. 2003; Mahmoudian et al. 2004).

Typical *MEMS* devices employ a parallel capacitor of which one electrode is fixed and the other is attached to a microcantilever or microbeam. The unfixed electrode is a massive (compare to the mass of the microbeam) microplate capable to vibrate by using the flexibility of the microbeam. The microplate serves as a mechanical resonator. It is actuated electrically and its motion can be controlled and detected by capacitive changes. The fundamental resonant frequency of the vibrating microelement is sensitive to the strain and shifts with external loads. The shift can be converted to an electric signal in the capacitor, and can be utilized to measure the cause of external load (Younis et al. 2003). These microbeam systems have quite a wide range of application as sensors and actuators. They can be utilized to create highly sensitive force and mass sensors. These structures are also utilized in

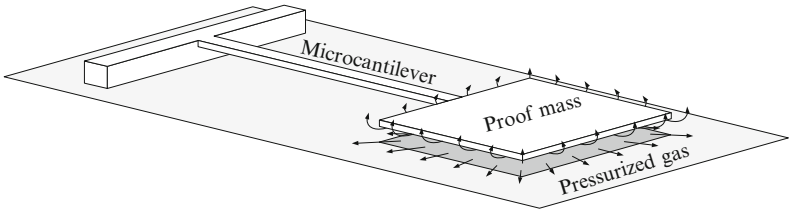

Fig. 2.1 A microcantilever resonator and resistance of the pressurized gas

atomic force microscopy (*AFM*) and scanning probe microscopy (*SPM*), which can probe extremely small features with a high resolution. These microbeams can also be integrated into *MEMS* flow, pressure, and biochemical sensors (Gupta et al. 2003).

Squeeze-film refers to thin-layer gas between the microplates of the capacitor as is shown in Fig. 2.1. The analysis of this phenomenon usually employs the Reynolds equation for isothermal incompressible fluid film. Isothermal equation makes it independent of the thermal effects. Finite element methods also make another basis to study the squeeze-film phenomena. However, finite element method approach, especially commercial software has problem to tackle with the nonlinear effects of many physical parameters (Younis et al. 2003; Younis 2004). There exist both, damping and stiffness factors in the squeeze-film phenomena. The factors arise from the effects of the surrounding gas medium. The damping factors are related to the way in which energy is transfer to the gas medium through thermal effects. Therefore, the quality factor of the cantilevers will be affected by squeeze-film damping effects. The stiffness factor, however, appears because the air under the microplate is acting similar to a visco-elastic member that would exhibit resistance to compression. In special circumstances, this would cause an increase in the effective spring constant of the system, which would outweigh the added damping effects and actually shift the resonant frequency up at increasing pressures (Yang et al. 1997a; Yang and Senturia 1997b; Yang 1998; Younis 2001; Harmany 2003).

Many studies have been reported in the late 20th and the begining of 21st century on squeeze-film damping, most notably by Starr (1990); Andrews et al. (1993); Andrews and Harris (1995); Yang and Senturia (1996); Yang et al. (1997a); Yang and Senturia (1997b); Veijola et al. (1998); Veijola and Mattila (2001); Abdel-Rahman et al. (2002); Younis et al. (2003). Analytical studies are based almost exclusively on a linearized form of the Reynolds equation, solutions to which have been derived for rectangular and circular geometries under the simplified boundary condition that the acoustic pressure vanishes at the structure's perimeter (Langlois 1962; Griffin et al. 1966; Blech 1983). Modifications to the equation have been made to account for more realistic boundary conditions (Darling et al. 1998) as well as slip flow at the solid–fluid interface (Sun et al. 2002) and the inclusion of

damping holes in the proof mass (Bao et al. 2003). Nonetheless, analytical solutions are inherently limited to simple geometries and numerical approaches are required to model more complex structures (Houlihan and Kraft 2005). In Chen and White (2000) and Chen and Kang (2000), the system first linearizes around an equilibrium point, and then extracts a subspace for reduced-order modeling. The states of the initial nonlinear system are projected onto the reduced state space.

Nayfeh and Younis (2004a,b) and Abdel-Rahman et al. (2004) have provided a very well and extensive review and analysis on the attempts for expressing the effects of squeeze-film in *MEMS* dynamics simulating the squeeze-film effect on a microbeam with an externally distributed pressure.

From a mathematical modeling viewpoint, most of the previous modeling have come up with equivalent mass, spring, viscosity, or damping affected by squeeze-film. Among them, Zhang et al. (2004) is a notable, where the authors have tried to model a clamped–clamped microbeam under two external loads; the electric and distributed squeezed film pressure. Assuming that the pressure is governed by the isothermal incompressible Reynolds equation they solved the problem using a Fourier series approach. It means they assumed a linear electric force. They modeled the effects of squeeze-film, by defining an effective mass and effective damping parameters called squeeze inertia and squeeze damping numbers expressed by two complicated series. Then the squeeze numbers were used in an equivalent linear mass-spring-dashpot resonator. Their analysis and approach has the shortcoming of assuming a linear electric force. The squeeze-film has no apparent effect within the order of displacements that the electric force may be assumed linear.

There have been several works which have dealt with the steady-state oscillation of such parametric and externally forced microbeams. The modeling and application of microbeam-based *MEMS* are described in some references such as Younis et al. (2003); Younis and Nayfeh (2003); Younis (2001, 2004); Malatkar (2003); Najar et al. (2005), using different viewpoints. However, the effects of slowly varying quantities in microbeams-based MEMS have not been fully investigated; specifically, when the unperturbed system contains a homoclinic manifold, which separates regions of qualitatively different behaviors. Nayfeh and co-workers have studied electrically actuated clamped–clamped microbeams in capacitive microswitches subject to a full nonlinear model (Abdel-Rahman et al. 2004, 2002; Zhao et al. 2004; Vogl and Nayfeh 2005; Nayfeh et al. 2005; Younis and Nayfeh 2005a,b). They focused on the damping mechanisms in microbeams (Nayfeh and Younis 2004a,b), and showed that squeeze-film and thermoelastic damping are the main sources of damping in microbeams vibration. Thermo-elastic effect is usually modeled by an equivalent viscous damping, while the squeeze-film phenomenon is analyzed by a coupled elesto-fluid problem.

The analysis of electric actuated microresonators often proceeds by abridging the system to a linearly damped Mathieu equation, with or without a synchronized forcing term. Then the resonance conditions of the equation are approximated and

carried out using the Mathieu stability diagram. Although such an analysis might be valid on short timescales within a small domain of control parameter space in the vicinity of primary resonance, the long-term behavior of the system can show significant differences. Even if the critical frequency ratios are assumed to be known a priori, these assumptions can fail to account for qualitative changes in the dynamical behavior of the system.

We present two mathematical models to simulate stiffness and damping effects of squeeze-film. Having a mathematical description simplifies the analysis and provides the power of prediction. A reliable mathematical model provides the ability to develop prototypes and design the best performance. Squeeze-film phenomena in microresonators provide mechanisms by which the system can undergo unexpected and undesired qualitative changes in their dynamical behavior and lose their functionality. However, inclusion of these phenomena can improve the design and functionality of microresonators.

2.2 Mathematical Modeling of Microresonators

2.2.1 Reduced-Model of Microresonators

Electrostatic actuation is achieved by applying a voltage difference between opposite electrodes of the variable capacitor. The induced electrostatic force deforms the capacitor until they are balanced by the restoring mechanical forces. The electric load is composed of a direct current (DC) polarization voltage, v_{p}, and an alternative current (AC) actuating voltage. Polarization voltage v_{p}, makes the system more complicated with interesting behaviors, and probably more effective and controllable microresonators. Electrostatic force of polarization voltage introduces *collapse load* or *pull-in* effect, where the mechanical restoring force of the microbeam can no longer resist the opposing electric forces. So a continuous increase in deflection occurs that leads to a short circuit in the electric field (Younis 2004). The polarization voltage controls the position and stability of equilibria. More specifically, the position and stability behavior of the origin is important, since it is to be act as the center of oscillation. It becomes unstable for large values of the polarization voltage v_{p}, but because of nonlinearity and excitation, as soon as the resonance causes the amplitude to increase, period dependency of the amplitude causes the resonance to detune and decrease its tendency to produce large amplitude. In other words, nonlinearity helps to limit the amplitude at resonance. A fact that will not be seen in the linearized model and will be shown in the following sections.

Analysis shows that electric force affects the restoring force with a softening effect. Therefore, the electric force tends to shift the natural frequencies to lower values. One-dimensional electrostatic force, f_{e}, per unit length of the beam is

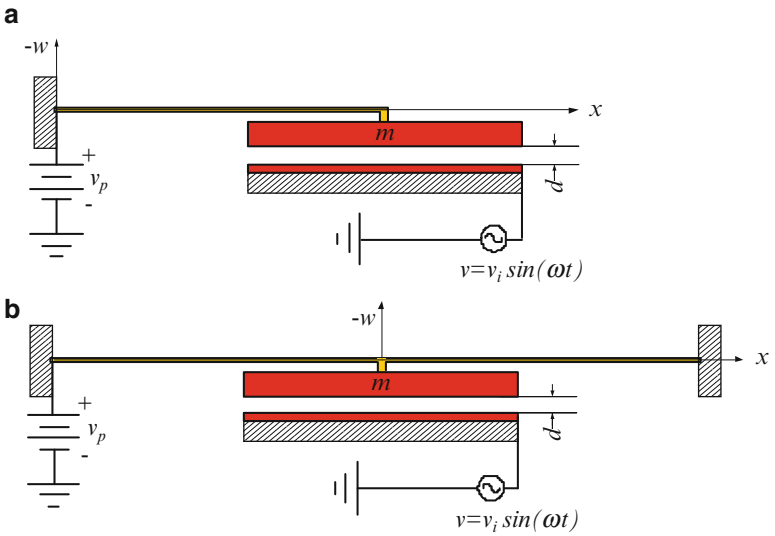

Fig. 2.2 A microcantilever and a clamed-clamped model of microresonator to keep the capacitor's plates parallel

$$f_{\mathrm{e}} = \frac{\varepsilon_0 a \left(v - v_{\mathrm{p}}\right)^2}{2\left(d - w\right)^2} \tag{2.1}$$

$$v = v_i \sin \omega t, \tag{2.2}$$

where $\varepsilon_0 = 8.854187817620 \times 10^{-12}\,\mathrm{A^2\,s^4/\,kg\,m^3}$ is permittivity in vacuum, A is the area of the microplate, and $w = w(x,t)$ is the lateral displacement of the microbeam. The complete microresonator is composed of a beam resonator, a ground plane underneath, and one (or more) capacitive transducer electrode/s. A DC-bias voltage, v_{p} , is applied to the resonator while an AC excitation voltage is applied to its underlying ground plane/s. A single capacitor clamped–clamped and a cantilever model of the resonator are illustrated in Fig. 2.2.

The inertia force per unit length of a vibrating microbeam is $f_i = \rho \frac{\partial^2 w}{\partial t^2}$, where ρ is the mass per unit length. Bending, axial force, and mid-plane stretching are the restoring forces in microbeams flexing. The mechanical restoring forces of microbeams are usually hardening and therefore, they tend to shift the natural frequencies to higher values. The restoring force due to rigidity of the microbeam is $f_{\mathrm{r}} = EI \frac{\partial^4 w}{\partial x^4}$ and the restoring force due to internal tension of the microbeam is $f_{\mathrm{t}} = P \frac{\partial^2 w}{\partial x^2}$. However, the internal tension force, P, is because of the increasing the length due to deflection mid-plane stretching $PL/\left(Ea_0\right) = \delta = \int (\mathrm{d}s - \mathrm{d}x) \approx \frac{1}{2}\int_0^L \left(\frac{\partial w}{\partial x}\right)^2 \mathrm{d}x$ (Esmailzadeh et al. 1997; Nayfeh and Mook 1979).

The viscous damping $f_v = c\frac{\partial w}{\partial t}$ is the most common sources of energy dissipation. However, viscous damping is usually a substitution for internal, thermal, structural, intrinsic and squeeze-film dampings. In order to analyze squeeze-film damping, we assume no such equivalent viscous damping is present.

2.2.2 Modeling the Squeeze Film Phenomena

Generally speaking, the efficiency of actuation and the sensitivity of motion detection of the microresonators improves by decreasing the distance between the capacitor electrodes, and increasing the effective area of the electrodes (White 2002; Lyshevski 2001; Zhang et al. 2004). Under these conditions, the squeeze-film phenomena appear if the *MEMS* device is not in a vacuumed capsule. Although a vast amount of microresonators are fabricated to operate in a partially vacuumed capsule, there are still a lot of applications that the resonator must work in direct contact with air or other fluids (White 2002). Squeeze-film phenomena are the result of the massive movement of the fluid underneath the plate, which is resisted by the viscosity of the fluid. A non-uniform pressure distribution gives rise underneath the movable plate, which acts as a spring and a damper. The equivalent spring and damping rates are dependent on the frequency and amplitude of oscillation. It is estimated that the damping force is more important at low frequencies, whereas the spring force is more significant at high frequencies (Nayfeh and Younis 2004a,b).

To analyze the squeeze-film effects, the non-uniform pressure distribution of the gas film may be added as an external force to the equation of lateral motion of the microbeam. The pressure, which is dependent on the distance between electroplates, must then be found using fluid dynamics. Hence, the phenomenon is a coupled elasto-fluid problem. Some researchers have used the incompressible isothermal Reynolds equation to solve the coupled elasto-fluid problem approximately (Younis and Nayfeh 2003; Nayfeh and Younis 2004a,b; Shi et al. 1996; Zhang et al. 2004; Hung and Senturia 1999). Using this approach, the squeeze-film load is evaluated by the resultant of the pressure distribution $f_p = \int_{-b/2}^{b/2} p \, \mathrm{d}y$, and pressure is calculated using Reynolds equation $\nabla \cdot \left[w^3 p \nabla p\right] = \eta \frac{\partial (pw)}{\partial t}$ where, $\eta = 12\mu/(1 + 6K)$ is the effective viscosity (Burgdorfer 1959; Yang 1998), K is the Knudsen number, and b is the width of the microelectrode plate (Younis 2004; Lyshevski 2001; Rewienski 2003). A better analysis for squeeze-film effects might be coupling the oscillating system with heat convections to make an elasto-thermo-fluid problem, and utilizing compressible and non-isothermal fluid dynamics. However, such an analysis would be time consuming, cumbersome, and case dependent and in general does not provide general rules of design for such systems.

Therefore, micromresonator devices obey a complex set of equations that must account for the tight coupling of multiple energy domains of the system. Direct solution of these equations based on fully meshed structures is computationally

intensive, making it difficult to use in system-level simulation. In order to perform rapid design prediction and optimization, accurate and easy-to-use reduced-order *MEMS* device models must be built (Chen et al. 2004). In order to overcome the high computational cost problem and thus to provide fast and efficient system level simulation, the *MEMS* design community has converged upon the technique of solving *MEMS* device dynamical behaviors by constructing low-order device models to match with the direct analysis. A common approach for doing this is based on parameterized lumped element representation for *MEMS* devices (Mukherjee et al. 1999).

When the beam bends, the pressure distribution of the ambient air under the microplate increases. This pressure increase produces a backward pressure force that damps the beam motion. The dynamic behavior of this coupled electromechanical fluidic system can be modeled with the beam equation and the Reynold's squeeze-film damping equation (Hung and Senturia 1999; Gupta and Senturia 1997; Pan et al. 1998; Shi et al. 1996; Starr 1990; Yang and Senturia 1996; Younis 2004) as

$$\rho\frac{\partial^2 w}{\partial t^2}+c\frac{\partial w}{\partial t}+EI\frac{\partial^4 w}{\partial x^4}=\frac{Ea_0}{L}\left(\frac{1}{2}\int_0^L\left(\frac{\partial w}{\partial x}\right)^2\mathrm{d}x\right)\frac{\partial^2 w}{\partial x^2}+\int_{-b/2}^{b/2}p\,\mathrm{d}y+\frac{\varepsilon_0 a\left(v-v_\mathrm{p}\right)^2}{2\left(d-w\right)^2} \tag{2.3}$$

$$\nabla\cdot\left[w^3p\nabla p\right]=\frac{12\mu}{1+6K}\frac{\partial\left(pw_0\right)}{\partial t}, \tag{2.4}$$

where $w(x,t)$ is the height of the beam above the substrate, and $p(x,y,t)$ is the pressure distribution under the beam. (2.3) is distributed along the x-axis. Nominal value of the parameters involved are: beam length $L=610\mu$ m, width $b=40\mu$ m, thickness $h=2.2\mu$ m, initial gap $d=2.3\mu$ m, material Young's modulus $E=149G$ Pa, density $\rho/(hb)=2330\,\mathrm{kg/m^3}$, air viscosity $\mu=1.82\times10^{-5}\,\mathrm{kg/ms}$, moment of inertia $I=bh^3/12$, Kundsen's number $K=\kappa/w$, and the ambient air $P_a=1.013\times10^5$ Pa (Chen et al. 2004). The mean-free path of the gas $\kappa=0.064\mu$ m. The size and mass of the microplate is $a=150\times150\mu\,\mathrm{m^2}$ and $m=1.15\times10^{-10}$ kg. The effective viscosity η was under investigation for more than a century (Yang 1998), while determined by Burgdorfer (1959).

Equations (2.3) and (2.4) show that simulating the dynamic behavior of the device involves squeeze-film, mechanical and electrostatic components. The system is nonlinear due to the nonlinear nature of the squeeze-film force, nonlinear rigidity of mid-plane stretching, and the nonlinear electrostatic force. The Reynolds equation is a combination of the Navier–Stokes equation, the continuity equation, and the state equation Yang (1998). The derivation of the isothermal Reynolds equation starts with integrating the Navier–Stokes equation in y-axes, then obtaining mass flow equations which are functions of the pressure gradient in x and y directions. Then substituting the results into the continuity equation and obtain a

primitive form of the Reynolds equation, which is a function of density and, is temperature dependence. Under the assumption of isothermal conditions, we can further eliminate the density term by using the equation of state and thus obtain the isothermal Reynolds equation. The Reynolds equation derived under these assumptions:

1. The fluid is Newtonian.
2. The fluid obeys the ideal gas law.
3. The inertia and body forces are negligible compared to the viscous and pressure forces.
4. The variation of pressure across the fluid film is negligibly small.
5. The flow is laminar.
6. The width of the gap separating the two plates, where the gas is trapped inside, is very small compared to the lateral extent of the plates.
7. The fluid can be treated as continuum and does not slip at the boundaries.
8. The system is isothermal.

Since there are no analytical solutions to (2.3) and (2.4), some researchers necessarily solved the equations numerically under more simplifications. The Reynolds equation can be linearized around the ambient pressure and gap size (Nayfeh and Younis 2004a,b). Now, ignoring the nonlinearities in equation reduces the problem to a couple of linear partial differential equations, which can still be solved numerically only. Based on these assumption, it is estimated that the squeeze-film damping force is more important at low frequencies, whereas the squeeze-film spring force is more significant at high frequencies (Nayfeh and Younis 2004a,b).

In case of a rectangular parallel plate oscillating in normal direction with a given small harmonic motion, and the pressure boundary conditions on the edges of the plates are equal to ambient pressure, the analytical solutions of pressure force components of the linearized Reynolds equation are found by Blech (1983). However, in microresonator dynamic analysis, the displacement oscillation of the microbeam is what the analysis must find and therefore, the Blech analysis can only be used as a rough estimation.

2.2.2.1 Damping Model

We separate the two characteristics of the squeeze-film phenomena and model the damping and stiffness effects individually. Motion of the microplate and flow of the gas underneath is similar to the function of a decoupler plate in hydraulic engine mounts (Golnaraghi and Jazar 2001; Jazar 2002). More specifically, the squeeze-film damping is qualitatively similar to the function of decoupler plate in hydraulic engine mounts, which is an amplitude-dependent damping (Christopherson and Jazar 2005). It means squeeze-film damping effect is a positive

phenomenon to isolate the vibration of microplate from the substrate. Following Golnaraghi and Jazar (2001), and utilizing the aforementioned similarity, we model the squeeze-film damping force, f_{sd}, by a cubic function,

$$f_{sd} = c_s w^2 \frac{\partial w}{\partial t} \tag{2.5}$$

where the coefficient c_s is assumed constant and must be evaluated experimentally. The equation expresses a stiffness model because of the displacement term $\partial w/\partial t$, and it is nonlinear because the coefficient $\left(c_s w^2\right)$ of $\partial w/\partial t$ is displacement dependent. The equation expresses a damping model because of the velocity term $\partial w/\partial t$, and it is nonlinear because the coefficient $\left(c_s w^2\right)$ of $\partial w/\partial t$ is displacement dependent. The displacement dependency is of second degree to indicate that the damping coefficient approaches high values when the electrodes get close to each other. However, the amplitude of vibration is practically less than the gap size and hence, when the electrodes get close the speed approaches zero and makes squeeze-film damping zero. Considering these physical constraints and dynamic behavior of the damping, a general damping function can be

$$f_{sd} = c'_s \left(\frac{w}{d}\right)^{2i+2} \left(\frac{\partial w}{\partial t}\right)^{2i+1} \qquad i \in \mathbb{N} \tag{2.6}$$

where the function (2.5) is the simpest model.

2.2.2.2 Stiffness Model

In the simplest case, we present the following fifth degree function to simulate the spring force, f_{ss}, of the squeeze-film phenomenon, simply because at low amplitudes, $w \approx 0$, the fluid layer is not strongly squeezed and there is no considerable resistance. On the other hand, at high amplitudes, $w \approx d$, there is not much fluid to react as a spring. In addition, speed is proportionally related to the squeezeness of trapped fluid.

$$f_{ss} = k_s (d - w)^2 w \left(\frac{\partial w}{\partial t}\right)^2 \tag{2.7}$$

The coefficient k_s assumed constant and must be evaluated experimentally. The coefficients c_s and k_s are dependent on geometry as well as dynamic properties of the fluid, but assumed to be independent of kinematics of the microbeam such as displacement and velocity.

The equation expresses a stiffnes model because of the displacement term w, and it is nonlinear because the coefficient $k_s (d - w)^2 (\partial w/\partial t)^2$ is displacement and velocity dependent. The displacement dependency is of second degree to indicate that the stiffness coefficient approaches low values when the electrodes get close

to each other. It is velocity dependent to indicate that the stiffness effect of the film is higher at higher speeds and is zero at no speed. Considering these physical constraints and dynamic behavior of the stiffness, a general stiffness function can be

$$f_{ss} = k_s' \left(d - w\right)^{2i+2} \; w^{2i+1} \left(\frac{\partial w}{\partial t}\right)^{2i+2} \qquad i \in \mathbb{N} \tag{2.8}$$

where the function (2.7) is the simpest model.

2.3 Equation of Motion

Including mathematical modeling of squeeze-film effects, the following equation is to be utilized for dynamic analysis of the microresonator behavior using $w = w(x, t)$ for lateral displacement of a microbeam.

$$\begin{aligned} &\rho \frac{\partial^2 w}{\partial t^2} + EI \frac{\partial^4 w}{\partial x^4} + c_s w^2 \frac{\partial w}{\partial t} + k_s \left(d - w\right)^2 w \left(\frac{\partial w}{\partial t}\right)^2 \\ &= \frac{E a_0}{L} \left(\frac{1}{2} \int_0^L \left(\frac{\partial w}{\partial x}\right)^2 \mathrm{d}x\right) \frac{\partial^2 w}{\partial x^2} + \frac{\varepsilon_0 a \left(v - v_\mathrm{p}\right)^2}{2 \left(d - w\right)^2}. \end{aligned} \tag{2.9}$$

We define the following variables to make the equation of motion dimensionless. The parameter n is a constant depending on mode shape of the microbeam.

$$\tau = \omega_1 t \tag{2.10}$$

$$\omega_1 = \frac{n^2}{L^2} \sqrt{\frac{EI}{\rho}} \tag{2.11}$$

$$z = \frac{x}{L} \tag{2.12}$$

$$y = \frac{w}{d} \tag{2.13}$$

$$Y = \frac{w_0}{d} \tag{2.14}$$

$$r_x = \frac{\omega}{\omega_x} \tag{2.15}$$

$$r = \frac{\omega}{\omega_1} \tag{2.16}$$

$$a_1 = \frac{\varepsilon_0 a L^4}{2 d^3 EI} \tag{2.17}$$

$$a_3 = \frac{a_0 d^2}{I} n \tag{2.18}$$

$$a_4 = \frac{c_s d^2 L^2}{\sqrt{\rho E I}} \tag{2.19}$$

$$a_5 = \frac{k_s d^4}{\rho}. \tag{2.20}$$

Using these parameters, the equation of motion transforms to the following dimensionless equation.

$$\frac{\partial^2 y}{\partial \tau^2} + \frac{\partial^4 y}{\partial z^4} + a_4 y^2 \frac{\partial y}{\partial \tau} + a_5 (1-y)^2 y \left(\frac{\partial y}{\partial \tau}\right)^2 = a_3 \frac{\partial^2 y}{\partial z^2} \frac{1}{2} \int_0^1 \left(\frac{\partial y}{\partial z}\right)^2 \mathrm{d}z + a_1 \frac{(v - v_\mathrm{p})^2}{(1-y)^2}. \tag{2.21}$$

We apply a separation solution, $y = Y(\tau)\ \varphi(z)$, and assume a first harmonic function as the mode shape of the deflected microbeam. By accepting a first harmonic shape function, the temporal function $Y(\tau)$ would then represent the maximum deflection of the microbeam, which is the middle point for symmetric boundary conditions, and the tip point for microcantilever. Therefore, the differential equation describing the evolution of the temporal function $Y(\tau)$ would be

$$\ddot{Y} + Y + \lambda Y^3 + a_4 Y^2 \dot{Y} + a_5 (1-Y) Y \dot{Y}^2 = \frac{1}{(1-Y)^2} \left((\alpha + \beta) + 2\sqrt{2\alpha\beta} \sin(r\tau) - \beta \cos(2r\tau) \right), \tag{2.22}$$

where

$$\alpha = a_1 v_\mathrm{p}^2 \tag{2.23}$$

$$2\sqrt{2\alpha\beta} = 2 a_1 v_\mathrm{p} v_i \tag{2.24}$$

$$\beta = \frac{a_1}{2} v_i^2 \tag{2.25}$$

$$\lambda = n^2 a_3 \tag{2.26}$$

$$n^2 = \frac{1}{2} \int_0^1 \left(\frac{\partial \varphi}{\partial z}\right)^2 \mathrm{d}z. \tag{2.27}$$

The first harmonic mode shape to satisfy the required boundary conditions for a microcantilever is

$$\varphi(z) = 1 - \cos\left(\frac{\pi z}{2}\right) \tag{2.28}$$

and therefore,

$$n = \frac{\pi}{4}. \tag{2.29}$$

(2.22) is an effective and applied reduced model of the microresonator including the squeeze-film phenomena as well as geometric nonlinearities and exact electrostatic actuating force.

2.4 Initial Deflection

The cubic stiffness term in (2.22) is a result of mid-plane stretch. Let us assume mechanical restoring force is denoted by $f_m = Y + \lambda Y^3$, $0 \leq Y \leq 1$. Applying a polarization voltage affects the equilibrium positions of the system and bends the microbeam. Consequently, the rest position of the microbeam would not be at $Y = 0$. Assume the polarized *MEMS* has the rest point at $Y = Y_0$, $0 \leq Y_0 \leq 1$, instead of $Y = 0$. This will translate the origin of measuring f_m and introduces a new mechanical restoring force as $f_m = \left(1 - 3\lambda Y_0^2\right) Y - 3\lambda Y_0 Y^2 + \lambda Y^3$, $0 \leq Y \leq 1$. Therefore, a second degree restoring force must be added to the equations of motion to include the initial bending of the microbeam. Note that including second degree restoring force makes the system asymmetric, which generates its own problems when we try to solve the system using perturbations and other approximate methods. The initial displacement Y_0 is a function of polarization voltage and can be determined by searching for equilibria of the *MEMS*. The equilibria would be found by ignoring time variations in (2.22)

$$\left(1 + \lambda Y^2\right)(1 - Y)^2 Y = \alpha.$$

Polarization voltage and initial bending of the microbeam introduce a new problem. When the polarization voltage of the inactive *MEMS* is not zero, the clearance between the two plates of the capacitor would not be d, and therefore, the limit of Y would be less than 1. It might be better to redefine the equations in order to have the bent rest point always as a zero equilibrium position (Mahmoudian et al. 2004). In this case, the gap size, d, is a function of polarization voltage.

2.5 Mathematical Analysis

Steady-state response of the system can be utilized to determine the sensitivity of the steady-state response of the system to parameter variation, as well as frequency shifts and amplitude changes. As is seen from (2.22), nonlinearity is due to electrostatic actuation, mid-plane stretching, squeeze-film damping and squeeze-film stiffness. To clarify the effects of squeeze-film phenomena, we assume

the system is linear everywhere except for squeeze-film effects and we keep the squeeze-film stiffness and damping as presented in (2.5) and (2.7). This system is governed by the following forced nonlinear Mathieu equation.

$$\begin{aligned}\ddot{Y} &+ a_4 Y^2 \dot{Y} + a_5 (1-Y)^2 Y \dot{Y}^2 \\ &+ \left(1 - 2\left(\alpha + \beta + 2\sqrt{2\alpha\beta}\sin(r\tau) - \beta\cos(2r\tau)\right)\right) \\ &= \alpha + 2\sqrt{2\alpha\beta}\sin(r\tau) + 2\beta\sin^2(r\tau)\,. \end{aligned} \tag{2.30}$$

Following the averaging method, in order to find the amplitude of steady state oscillation of the microbeam around resonance and taking care of initial displacement due to polarization, we assume a solution in the following form

$$Y = A_0 + A(\tau)\sin(r\tau + \psi(t)) \tag{2.31}$$

$$\dot{Y} = A(\tau)\, r\cos(r\tau + \psi(t))\,. \tag{2.32}$$

These solutions are applied provided that

$$\dot{A}(\tau)\sin(r\tau + \psi(t)) + A(\tau)\,\dot{\psi}(t)\cos(r\tau + \psi(t)) = 0. \tag{2.33}$$

Substituting (2.31) and (2.32) in (2.30) leads to an equation, which must be utilized to find the secular term

$$A_0 = \frac{\alpha + \beta}{1 - 2\alpha - 2\beta} \tag{2.34}$$

That equation along with (2.33) must be used to derive a couple of first-order differential equations for $\dot{A}(\tau)$ and $\dot{\psi}(t)$, say

$$\dot{A}(\tau) = f_1(a_4, a_5, \alpha, \beta, r, A, \varphi) \tag{2.35}$$

$$A(\tau)\,\dot{\psi}(\tau) = f_2(a_4, a_5, \alpha, \beta, r, A, \varphi), \tag{2.36}$$

where

$$\varphi(\tau) = r\tau + \psi(\tau). \tag{2.37}$$

Assuming $\dot{A}(\tau)$ and $\dot{\psi}(\tau)$ are slow variables and their average remains constant during one cycle, we substitute their equations with their integral over one period of oscillation.

$$\begin{aligned} A(\tau) = \int_0^{2\pi} \dot{A}(\tau)\,\mathrm{d}\varphi = -\frac{\pi}{r}\left(\left(A_0^2 + \frac{A^2}{4}\right) rAa_4 + \beta A\sin 2\psi\right) \\ -\frac{\pi}{r} 2\sqrt{2\alpha\beta}\,(1 + 2A_0)\sin\psi \end{aligned} \tag{2.38}$$

$$\psi(\tau) = \int_0^{2\pi} \dot{\psi}(t)\,\mathrm{d}\varphi = \frac{\pi}{rA}\left(\left(1 + 3A_0^2 + \frac{A^2}{2} - \frac{A_0}{2}\right)A^3\frac{r^2}{4}a_5\right)$$
$$+A\left(1 - r^2 - 2\alpha - 2\beta - \beta\cos^2\psi\right)$$
$$-\frac{\pi}{rA}\left(2\sqrt{2\alpha\beta}\,(1 + 2A_0)\cos\psi\right). \tag{2.39}$$

At steady-state conditions, $A(\tau)$ and $\psi(\tau)$ must not vary in time and therefore, the left-hand sides of (2.38) and (2.39) are zero. Eliminating $\psi(\tau)$ provides a relationship between the parameters of the system to have a periodic steady-state response with frequency r.

$$Z_1 r^4 + Z_2 r^2 - Z_3 - (Z_4 + Z_5)\sqrt{Z_6} + Z_7 = 0. \tag{2.40}$$

The parameters Z_i, $i = 1, 2, \ldots, 16$, are dynamic parameters of the system and are independent of the excitation frequency.

$$Z_1 = a_5^2\beta^2A^8\left(A^4 + \left(12A_0^2 - 16A_0 - 4\right)A^2\right)$$
$$+4\left(1 + 9A_0^4 - 24A_0^3 + 22A_0^2 - 8A_0\right)$$
$$+16a_5\beta^2A^6\left(-A^2 - 6A_0^2 + 9A - 2\right) + 64\beta^2A^4 \tag{2.41}$$
$$Z_2 = 16a_5\beta^2A^6(2\beta + 2\alpha - 1)\left(-6A_0^2 + 8A_0 - A^2 - 2\right)$$
$$+4\beta^2A^8\left(a_4^2 + 8a_5\right) + 32\beta^2A^6\left(a_4^2A_0^2 + 2a_5\left(3A_0^2 + 4A_0 + 1\right)\right) \tag{2.42}$$
$$Z_3 = 64\beta^2A^4(1 - 4\alpha) - 256\beta^3A^2\alpha(2A_0 + 1)^2 \tag{2.43}$$
$$Z_4 = 128\beta^2A^2A_0\sqrt{2\alpha\beta} \tag{2.44}$$
$$Z_5 = 64\beta^2A^2\sqrt{2\alpha\beta} \tag{2.45}$$
$$Z_6 = a_5\beta A^4r^2\left(2 + 6A_0^2 + A^2 - 8A_0\right) + 32\alpha\beta A_0(1 + A_0)$$
$$+8\alpha\beta\left(1 - 2A^2\right) + 8\beta A^2\left(1 - r^2 - \beta\right) \tag{2.46}$$
$$Z_7 = 64\beta^2A^4\left(8\alpha\beta + 3\beta^2 - 4\beta + 4\alpha^2\right). \tag{2.47}$$

Note that nonzero excitation is necessary to have a nontrivial response. The effect of variation of each parameter on the dynamic response of the *MEMS* will be examined in the next section. Since the frequency response equation cannot be solved for any parameters, a numerical analysis is needed to evaluate the overall effect of parameters. In what follows, the analytic description (2.40) is utilized to describe the behavior of steady-state dynamic of the system around resonance.

2.6 Dynamic Analysis

The steady-state response of microresonators reflect important behavior of resonator-based *MEMS*. The resonance frequency determines the amount of force the structure can exert while the frequency response establishes the pick amplitude of oscillation. These characteristics indirectly affect design parameters such as sensitivity, quality factor, switching frequency, and external noise (Sudipto and Aluru 2004). Amplitude of oscillation of the microresonator at steady-state conditions is determined by (2.40) indicating that its dynamics governs by polarization voltage parameter α, alternative excitation voltage parameters β, the excitation frequency ratio r, as well as the squeeze-film damping and stiffness parameters a_4, and a_5. In order to demonstrate the dependency of steady-state behavior of the *MEMS*, we graphically illustrate the frequency response for various parameters. The nominal values of a sample microcantilever and adapted from Yang et al. (2002); Khaled et al. (2003), although because of the dimensionless forms of the equations, any other microresonator can be analyzed as well.

Figures 2.3–2.6 depicts the effect of variation of polarization voltage for a set of parameters. The amplitude of steady-state oscillation increases by increasing the polarization voltage. Almost no squeeze-film effect is shown in Fig. 2.3, where a_4 is set to a small value and a_5 is set to zero. Since we eliminated every kind of damping except the squeeze-film damping, a small squeeze-film damping is needed to simulate dissipation mechanisms presented in the system. Low squeeze-film damping is similar to viscous damping and shows no nonlinear effects qualitatively. Squeeze-film stiffness affects the restoring force of the system in a nonlinear fashion as shown in Fig. 2.4. This effect is important for resonator mass sensors which have been analyzed and designed by assuming constant stiffness. Increasing the damping diminishes the response of the system and dominates the nonlinear

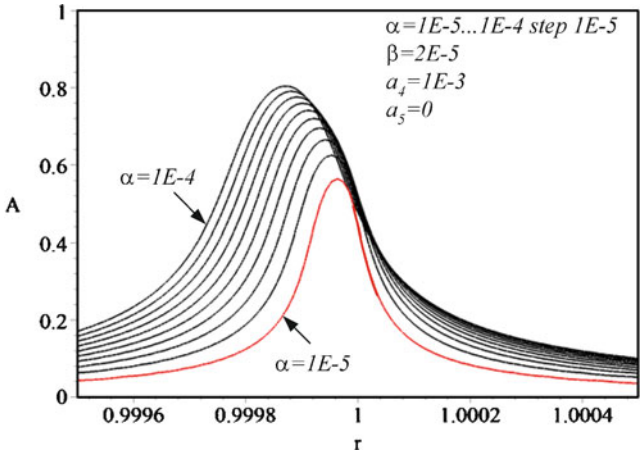

Fig. 2.3 Effect of variation of polarization voltage on frequency response of the microbeam

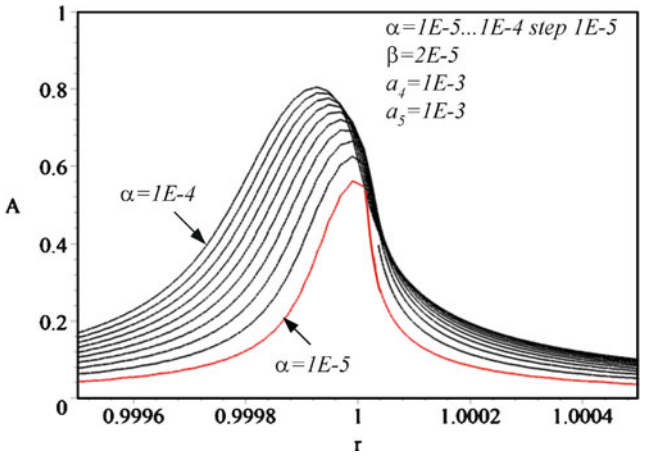

Fig. 2.4 Effect of variation of polarization voltage on frequency response of the microbeam

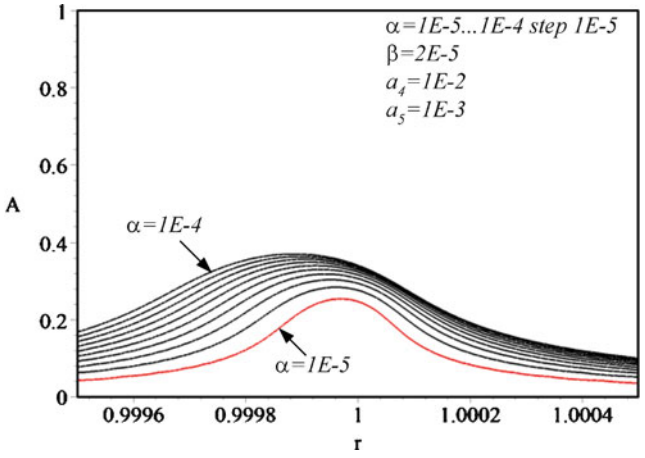

Fig. 2.5 Effect of variation of polarization voltage on frequency response of the microbeam

effects of little stiffness. This effect is shown in Fig. 2.5. Figure 2.6 shows the frequency response of the microbeam with a little damping and a high squeeze-film stiffness effects. It shows that squeeze-film stiffness shifts the resonance to higher frequencies and can introduce a resonance amplitude dependency as well as jump and instability occurrence. The peak value of the frequency response at resonance is a monotonically increasing function of the polarization voltage. Therefore, there must be a maximum acceptable α, due to constraint $Y < 1$.

It is shown in Figs. 2.7–2.10 that the response of the system to variation of the excitation voltage has the same pattern as changing the polarization voltage.

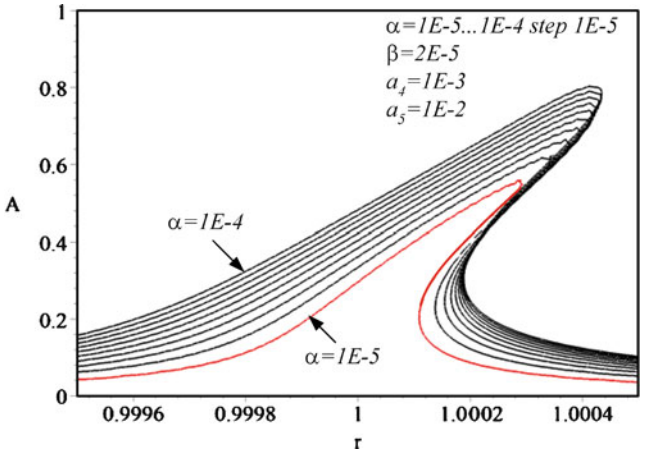

Fig. 2.6 Effect of variation of polarization voltage on frequency response of the microbeam

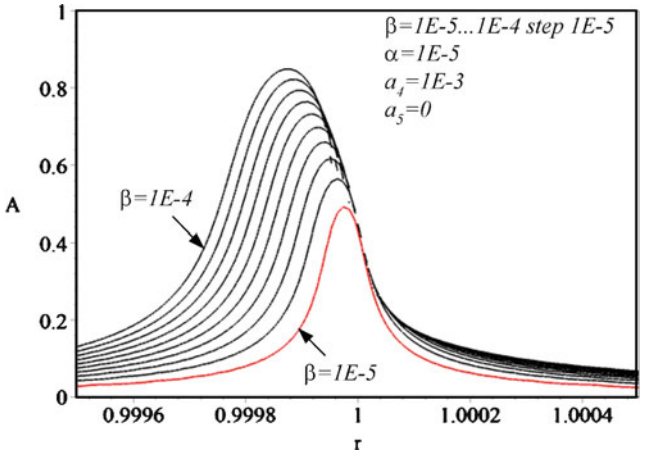

Fig. 2.7 Effect of variation of excitation voltage on frequency response of the microbeam

More specifically, the peak value increases and the resonant frequency shifts to higher frequencies when the amplitude of the excitation voltage increases. Squeeze-film damping and stiffness also have the same effects as described for polarization voltage variation. There must also be a higher limit for the excitation voltage to have oscillation within the gap size limit.

Variation of the squeeze-film damping is illustrated in Figs. 2.11and 2.12. Increasing damping diminishes the amplitude of the oscillation as expected. It is known that decreasing the damping increases the quality factor of the system and is not considered a positive phenomenon. Therefore, damping has two main roles in *MEMS* dynamics. It should exist to control the system to stay within the physical

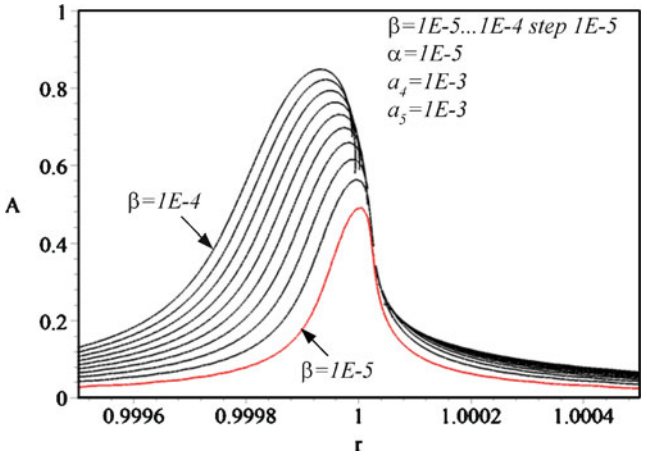

Fig. 2.8 Effect of variation of excitation voltage on frequency response of the microbeam

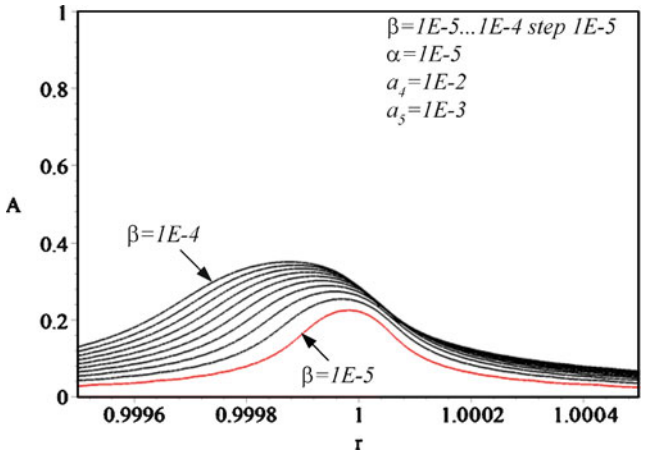

Fig. 2.9 Effect of variation of excitation voltage on frequency response of the microbeam

limit $Y < 1$; and on the other hand, it must be as low as possible to provide high quality factor (Younis 2004). In Fig. 2.11, the squeeze-film stiffness is ignored, while there is some stiffness in Fig. 2.12. The effect of backbone tilting is obvious when squeeze-film stiffness is present.

Variation of the squeeze-film stiffness, which is equivalent to oscillating in a viscouser media, is shown in Figs. 2.13 and 2.14. Comparing Figs. 2.13 and 2.14 indicates that introducing damping reduces the pick amplitude but keeps the qualitative behavior of the system. Variation of the stiffness has almost no or little effect on the pick amplitude; however, bending the backbone curve is a significant effect. Hence, there must be a maximum allowable stiffness to avoid jump.

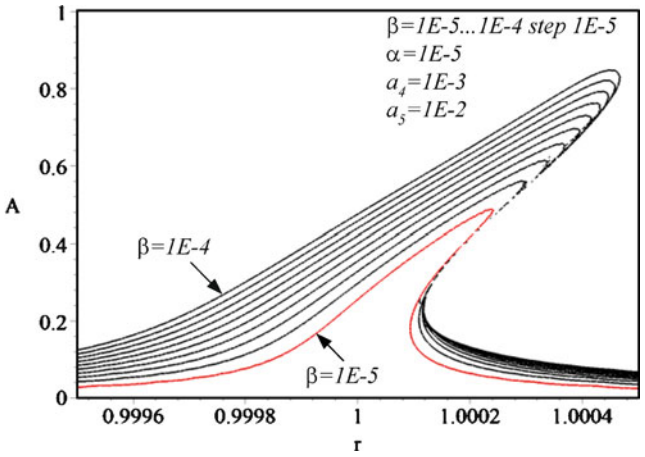

Fig. 2.10 Effect of variation of excitation voltage on frequency response of the microbeam

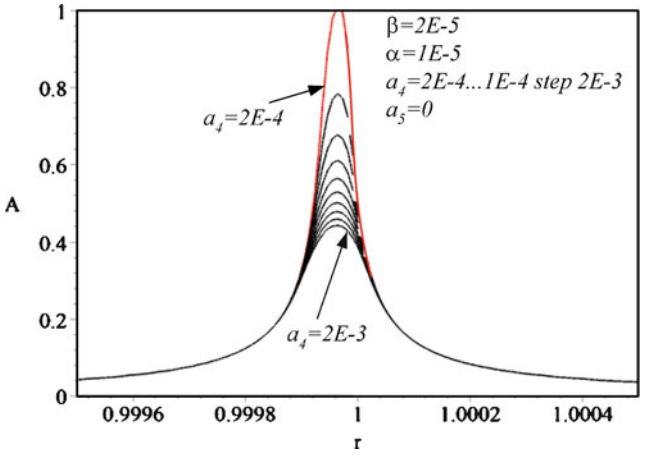

Fig. 2.11 Effect of variation of squeeze-film damping on frequency response of the microbeam

Frequency response analysis has shown that the squeeze-film stiffness has the most impact on resonance frequency and affects as a hardening spring. However, polarization and excitation voltages also have a softening effect and shift the resonance frequency to lower values. On the other hand, squeeze-film damping has high effects on decreasing the peak amplitudes with least affect on resonance frequency shift.

The presented model cannot be validated without looking at the equivalent linear damping and stiffness of the model. In other words, the most important fact showing the proposed dynamic can model the squeeze-film phenomena effectively is the

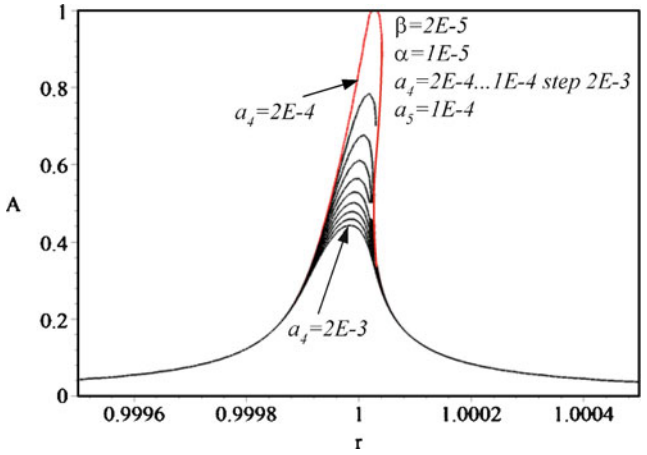

Fig. 2.12 Effect of variation of squeeze-film damping on frequency response of the microbeam

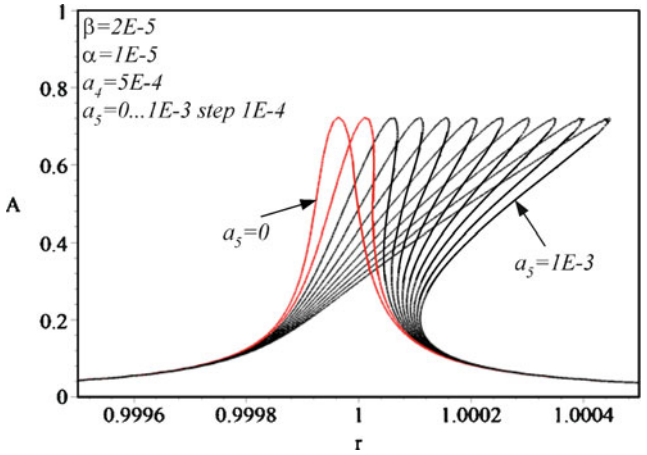

Fig. 2.13 Effect of variation of squeeze-film damping on frequency response of the microbeam

equivalent linear stiffness and damping, predicted for the first time by Blech (1983). Figures 2.15–2.16 depict the equivalent damping and stiffness, where k_{eq}, and c_{eq} are traditional linear stiffness and damping per unit length of the microbeam. The equivalent stiffness k_{eq}, and damping c_{eq}, are evaluated numerically by comparing the frequency response of the modeled microresonator with a microresonator having linear damping and stiffness. The equivalent damping is illustrated in Fig. 2.15 and the equivalent stiffness is depicted in Fig. 2.16. The results are quite comparable and in agreement with what presented by Blech (1983). The squeeze-film stiffness

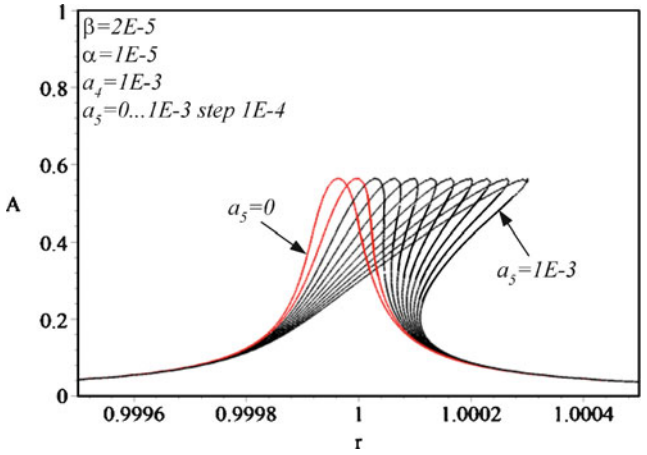

Fig. 2.14 Effect of variation of squeeze-film damping on frequency response of the microbeam

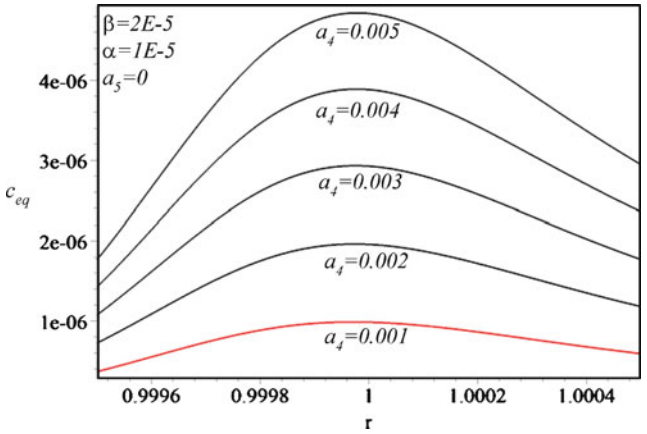

Fig. 2.15 Equivalent linear damping and stiffness as a function of frequency and squeeze-film damping and stiffness coefficients

k_s and damping c_s coefficients, hidden in a_5 and a_4, are proportional to their linear equivalents k_{eq} and c_{eq}. The equivalent squeeze-film damping is higher around resonance and decreases beyond that, justifying a decreasing effect on resonant amplitude. However, the equivalent squeeze-film stiffness is a monotonically increasing function of both frequency and squeeze-film stiffness coefficient. Therefore, stiffness has more effect at high frequencies, while damping affects the system at low and resonance frequencies.

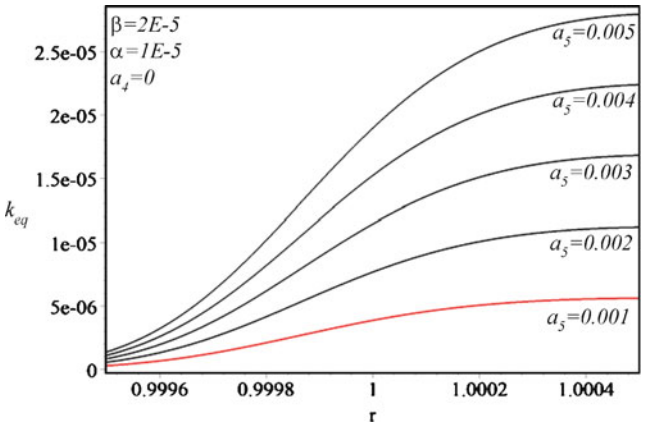

Fig. 2.16 Equivalent linear damping and stiffness as a function of frequency and squeeze-film damping and stiffness coefficients

2.7 Conclusion and Future Work

This work introduces a mathematical model to simulate the effects of squeeze-film phenomena on dynamics and performance of microbeam-based electromechanical resonators. Squeeze-film phenomena, also referred to as "squeeze-film damping," strongly influence the performance of microelectro-mechanical systems, and therefore is an important parameter to be considered in design and control of such systems. To improve the efficiency of actuation and sensitivity, the gap between the capacitor plates is usually kept minimized creating more squeeze-film resistance to the motion of the microplate in the viscous fluid. The squeeze-film damping is a deep-rooted multidisciplinary subject in dynamics of thermo-fluid-solid interactions. In this research, the squeeze-film parameters are modeled by two functions in terms of equivalent damping and the overall stiffness of the system. The changes in the stiffness and damping forces, which are, respectively, modeled by a fifth and a third degree nonlinear functions, are assumed to be frequency and amplitude dependent.

The dynamics model for microresonators focusing on modeling of the impacts due to squeeze-film in performance of such systems is analyzed utilizing a dimensionless equation of motion and employing averaging perturbation method. The frequency-amplitude relationship of the system is presented by an implicit equation. A sensitivity analysis has been performed to illustrate the effect of the phenomena in steady-state response, frequency shift, and pick amplitude of the oscillation. It is shown that the damping has little effect on resonant shift but diminishes the pick amplitude of oscillation significantly. The nonlinear characteristic of the stiffness model affects the steady-state dynamic behavior of the system dramatically. Due to hardening behavior, the backbone of the frequency response bends to higher frequencies and introduces jump in high values. Validation of the model has

been done solely by evaluating the equivalent frequency-dependent stiffness and damping. It was shown that the behavior of such equivalent coefficients qualitatively match with reported results. The mathematical modeling is consistent to enhance the exploration as well as design and control of *MEMS* more effectively.

To show the direction of next steps in improvement of the presented theory, it should be noted that the development of the dynamics model and the theoretical sensitivity analysis needs to be along with conduction of proper experiments. Note that the presented models do not necessarily require micro-scale systems to be applied. Hence, the model can be confirmed and coefficients may be evaluated utilizing a meso scale resonator, although the squeeze-film phenomena are significant in micro scale. Dynamics of microresonators must also be examined under the effect of squeeze-film phenomenon in time space to analyze and validate transient responses. The introduced coefficients, which are assumed to be independent of the frequency and amplitude of oscillation, must be determined for individual cases to determine its dependency to the viscosity of media, as well as geometry of the microbeam. In the presented analysis, the nonlinearities of the flexural rigidity and electrostatic forces are ignored to clarify the influence of the squeeze-film phenomena. In another attempt, these nonlinearities must be included to be compared with the effects of phenomena.

2.8 Key Symbols

a_i Dimensionless parameters of equation of motion
a Effective area of electrode plate
a_0 Cross-sectional area of the beam
A Amplitude
A_0 Initial deflection
b Width of the microbeam
c Viscous damping rate
c_s Thermal damping force coefficient
d Gap size
E Young modulus
f_e Electric force
f_i Inertia force
f_m Mechanical restoring force
f_r Bending restoring force
f_{sd} Squeeze-film damping force
f_{ss} Squeeze-film stiffness force
f_t Tension force
f_v Viscous damping force
f_{Td} Thermal damping force

f_{Ts} Thermal stiffness force
f_{v} Viscous damping force
h Thickness of microbeam and microplate
I Cross-sectional second moment
K Knudsen number
k_s Squeeze-film stiffness force coefficient
l Linear dimension
l_T Thermal diffusion length
L Length of microbeam or microcantilever
m Mass
n Mode shape parameter
P Longitudinal internal tension force
r Dimensionless excitation frequency
s Curved beam length
t Time
v_{p} Polarization voltage
V Volume
w Lateral displacement
w_0 Maximum lateral displacement
x Longitudinal coordinate
x_0 Initial longitudinal stretch
x_d Dynamic longitudinal stretch
y Lateral coordinate, dimensionless lateral displacement
Y Dimensionless amplitude of oscillations at maximum
z Longitudinal dimensionless coordinate
Z Short notation parameter

Greek
α Polarization voltage parameter
β Alternative voltage parameter
μ Viscosity
λ Coefficient of cubic mechanical stiffness force
η Thickness of microplate
κ Conductivity
φ Mode shape function
ψ Phase angle
ε_0 Permittivity in vacuum
τ Dimensionless time

Symbol
overdot $\mathrm{d}\,()\,/\mathrm{d}t$

References

Abdel-Rahman EA, Nayfeh AH, Younis MI (2004) Finite amplitude motions of beam resonators and their stability. J Comput Theoret Nanosci 1(4):385–391

Abdel-Rahman EM, Younis MI, Nayfeh AH (2002) Characterization of the mechanicsl behavior of an electrically actuated microbeam. J Micromech Microeng 12:759–766

Andrews M, Harris I, Turner G (1993) A comparison of squeeze-film theory with measurements on a microstructure. Sensors Actuators A 36:79–87

Andrews MK, Harris PD (1995) Damping and gas viscosity measurements using a microstructure. Sensors Actuators A 49:103–108

Bao M, Yang H, Sun Y, French PJ (2003) Modified Reynolds equation and analytical analysis of squeeze-film air damping of perforated structures. J Micromech Microeng 13:795–800

Blech JJ (1983) On isothermal squeeze-films. J Lubric Technol 105:615–620

Burgdorfer A (1959) The influence of the molecular mean free path on the performance of hydrodynamic gas lubricated bearing. J Basic Eng 81:94–99

Chen J, Kang SM (2000) An algorithm for automatic model reduction of nonlinear MEMS devices. Proceedings of IEEE International Symposium Circuits and Systems, 28–31 May 2000, pp 445–448

Chen J, Kang S, Zou J, Liu C, Schutt-Ainé JE (2004) Reduced-order modeling of weakly nonlinear MEMS devices with Taylor-series expansion and Arnoldi approach. J Microelectromech Syst 13(3):441–451

Chen Y, White J (2000) A quadratic method for nonlinear model order reduction. Proceedings of the International Symposium on Modeling and Simulation of Microsystem Conference, March 2000

Christopherson J, Jazar GN (2005) Optimization of classical hydraulic engine mounts based on RMS method. J Shock Vibr 12(12):119–147

Darling RB, Hivick C, Xu J (1998) Compact analytical modeling of squeeze-film damping with arbitrary venting conditions using a green's function approach. Sensors Actuators A 70:32–41

Esmailzadeh E, Mehri B, Reza NJ (1997) Existence of periodic solution for equation of motion of simple beams with harmonically variable length. J Vibr Acoustics 119:485–488

Fedder GK (1994) Simulation Micromech Syst Ph.D. dissertation, University of California at Berkeley

Golnaraghi MF, Jazar RN (2001) Development and analysis of a simplified nonlinear model of a hydraulic engine mount. J Vibr Control 7(4):495–526

Griffin WS, Richardson HH, Yamanami S (1966) A study of fluid squeeze-film damping. ASME J Basic Eng D 88, 451–456.

Gupta A, Denton JP, McNally H, Bashar R (2003) NovelFabrication method for surface micromachined thin single-crystal silicon cantilever beams. J Microelectromech Syst 12(2):185

Gupta RK, Senturia SD (1997) Pull-in time dynamics as a measure of absolute pressure. Proceedings of the tenth annual international workshop on micro electro mechanical systems, New York, NY, pp 290–294

Harmany Z (2003) Effects of vacuum pressure on the response characteristics on MEMS cantilever structures. NSF EE REU PENN STATE Ann Res J I:54–64

Houlihan R, Kraft M (2005) Modeling squeeze-film effects in a MEMS accelerometer with a levitated proof mass. J Micromech Microeng 15:893–902

Hung ES, Senturia SD (1999) Generating efficient dynamical models for microelectromechanical systems from a few finite element simulation runs. J Microelectromech Syst 8:280–289

Jazar RN, Golnaraghi MF (2002) Nonlinear modeling, experimental verification, and theoretical analysis of a hydraulic engine mount. J Vibr Control 8(1):87–116

Khaled ARA, Vafai K, Yang M, Zhang X, Ozkan CS (2003) Analysis, control and augmentation of microcantilever deflections in bio-sensing systems. Sensors Actuators B 7092:1–13

Langlois WE (1962) Isothermal squeeze-films. Q Appl Math 20:131–150

Lyshevski SE (2001) Nano- and microelectromechanical systems, fundamentals of nano- and microengineering. CRC Press, Boca Raton, Florida

Madou MJ (2002) Fundamentals of microfabrication: the science of miniaturization, 2nd edn. CRC Press, Boca Raton, FL

Mahmoudian N, Aagaah MR, Jazar RN, Mahinfalah M (2004) Dynamics of a micro electro mechanical system (MEMS). International conference on MEMS, NANO, and smart systems, Banff, Alberta - Canada, 25–27 August 2004

Malatkar P (2003) Nonlinear vibrations of cantilever beams and plates. Ph.D. Thesis in Mechanical Engineering, Virginia Polytechnic Institute and State University

Mukherjee T, Fedder GK, Blanton RD (1999) Hierarchical design and test of integrated microsystems. IEEE Design Test 16:18–27

Najar F, Choura S, El-Borgi S, Abdel-Rahman EM, Nayfeh AH (2005) Modeling and design of variable-geometry electrostatic microactuators. J Micromech Microeng 15(3):419–429

Nayfeh AH, Mook DT (1979) Nonlinear oscillations. Wiley, New York

Nayfeh AH, Younis MI (2004a) Modeling and simulations of thermoelastic damping in microplates. J Micromech Microeng 14:1711–1717

Nayfeh AH and Younis MI (2004b) A new approach to the modeling and simulation of flexible microstructures under the effect of squeeze-film damping. J Micromech Microeng 14:170–181

Nayfeh AH, Younis MI, Abdel-Rahman EA (2005) Reduced-order modeling of MEMS. Third MIT conference on computational fluid and solid mechanics, Cambridge, MA, 14–17 June 2005

Pan F, Kubby J, Peeters E, Tan A, Mukherjee S (1998) Squeeze film damping effect on the dynamic response of a MEMS torsion mirror. J Micromech Microeng 8(3i):200–208

Rewienski MJ (2003) A trajectory piecewise-linear approach to model order reduction of nonlinear dynamical systems. Ph.D. thesis, Department of Electrical Engineering, Massachusetts Institute of Technology

Shi F, Ramesh P, Mukherjee S (1996) Dynamic analysis of micro-electro-mechanical systems. Int J Numer Meth Eng 39(24):4119–4139

Starr JB (1990) Squeeze-film damping in solid-state accelerometers. Proceedings of technical digest IEEE solid-state sensors and actuators workshop, Hilton Head Island, SC, pp 44–47

Sudipto K, Aluru NR (2004) Full-Lagrangian schemes for dynamic analysis of electrostatic MEMS. J Microelectromech Syst 13(5):737–758

Sun Y, Chan WK, Liu N (2002) A slip model with molecular dynamics. J Micromech Microeng 12:316–322

Veijola T, Mattila T (2001) Compact squeezed-film damping model for perforated surface. Proceedings of IEEE 11th international conference on solid-state sensors, actuators and microsystems, pp 1506–1509

Veijola T, Kuisma H, Lahdenper¨a J (1998) The influence of gas-surface interaction on gas-film damping in a silicon accelerometer. Sensors Actuators A 66:83–92

Vogl GW, Nayfeh AH (2005) A reduced-order model for electrically actuated clamped circular plates. J Micromech Microeng 15:684–690

White A (2002) Review of some current research in microelectromechanical systems (MEMS) with defence applications, DSTO Aeronautical and Maritime Research Laboratory, Fishermans Bend Vic, Australia, pp 10

Yang YJ (1998) Squeeze-film damping for MEMS structures. MS Thesis, Electrical Engineering, Massachusetts Institute of Technology

Yang YJ, Gretillat M-A, Senturia SD (1997) Effect of Air damping on the dynamics of nonuniform deformations of microstructures, international conference on solid-state. Sensors and Actuators. Chicago, 16–19 June 1997, pp 1094–1096

Yang JL, Ono T, Esashi M (2002) Energy dissipation in submicrometer thick single-crystal 116 cantilevers. J Microelectromech Syst 11(6):775–783

Yang Y-J, Senturia SD (1996) Numerical simulation of compressible squeezed-film damping. Proceedings of solid-state sensor and actuator workshop pp 76–79

Yang YJ, Senturia SD (1997) Effect of air damping on the dynamics of nonuniform deformations of microstructures. Proceedings of IEEE international conference on solid-state sensors and actuators, New York, NY, pp 1093–1096

Younis MI (2001) Investigation of the mechanical behavior of micro-beam-based MEMS devices. MS. thesis in Mechanical Engineering, Virginia Polytechnic Institute and State University, December 2001

Younis MI (2004) Modeling and simulation of micrielectromecanical system in multi-physics fields. Ph.D. thesis, Mechanicsl Engineering, Virginia Polytechnic Institute and State University

Younis MI, Abdel-Rahman EM, Nayfeh A (2003) A reduced-order model for electrically actuated microbeam-based MEMS. J Microelectromech Syst 12(5):672–680

Younis MI, Nayfeh AH (2003) A study of the nonlinear response of a resonant microbeam to electric actuation. J Nonlinear Dyn 31:91–117.

Younis MI, Nayfeh AH (2005a) Modeling squeeze-film damping of electrostatically actuated microplates undergoing large deflections. ASME 20th biennial conference on mechanical vibration and noise, 5th international conference on multibody systems, nonlinear dynamics and control, DETC2005-84421, Long Beach, CA, 24–28 September 2005

Younis MI, Nayfeh AH (2005b) Dynamic analysis of MEMS resonators under primary-resonance excitation. ASME 20th biennial conference on mechanical vibration and noise, DETC2005-84146, Long Beach, CA, 24–28 September 2005

Zhang C, Xu G, Jiang Q (2004) Characterization of the squeeze-film damping effect on the quality factor of a microbeam resonator. J Micromech Microeng 14:1302–1306

Zhao Z, Dankowicz H, Reddy CK, Nayfeh AH (2004) Modelling and simulation methodology for impact microactuators. J Micromech Microeng 14:775–784

http://www.springer.com/978-1-4614-1468-1

Nonlinear Approaches in Engineering Applications
Dai, L.; Jazar, R.N. (Eds.)
2012, XXXII, 536 p., Hardcover
ISBN: 978-1-4614-1468-1